Advances in Nano Research, *Vol. 7 No. 6 (2019) 405-417*
DOI: https://doi.org/10.12989/anr.2019.7.6.405

Cut out effect on nonlinear post-buckling behavior of FG-CNTRC micro plate subjected to magnetic field via FSDT

M. Jamali [1], T. Shojaee [1], B. Mohammadi [1] and R. Kolahchi*[2]

[1] *School of Mechanical Engineering, Iran University of Science and Technology, Tehran, Iran*
[2] *Institute of Research and Development, Duy Tan University, Da Nang 550000, Vietnam*

(*Received April 29, 2019, Revised July 9, 2019, Accepted August 3, 2019*)

Abstract. This research is devoted to study post-buckling analysis of functionally graded carbon nanotubes reinforced composite (FG-CNTRC) micro plate with cut out subjected to magnetic field and resting on elastic medium. The basic formulation of plate is based on first order shear deformation theory (FSDT) and the material properties of FG-CNTRCs are presumed to be changed through the thickness direction, and are assumed based on rule of mixture; moreover, nonlocal Eringen's theory is applied to consider the size-dependent effect. It is considered that the system is embedded in elastic medium and subjected to longitudinal magnetic field. Energy approach, domain decomposition and Rayleigh-Ritz methods in conjunction with Newton-Raphson iterative technique are employed to trace the post-buckling paths of FG-CNTRC micro cut out plate. The influence of some important parameters such as small scale effect, cut out dimension, different types of FG distributions of CNTs, volume fraction of CNTs, aspect ratio of plate, magnitude of magnetic field, elastic medium and biaxial load on the post-buckling behavior of system are calculated. With respect to results, it is concluded that the aspect ratio and length of square cut out have negative effect on post-buckling response of micro composite plate. Furthermore, existence of CNTs in system causes improvement in the post-buckling behavior of plate and different distributions of CNTs in plate have diverse response. Meanwhile, nonlocal parameter and biaxial compression load on the plate has negative effect on post-buckling response. In addition, imposing magnetic field increases the post-buckling load of the microstructure.

Keywords: nonlocal nonlinear post-buckling; FG-CNTRC micro rectangular cut out plate; first order shear deformation plate theory; Newton-Raphson iterative technique; magnetic field

1. Introduction

In recent years, researchers incline to study structures which have high mechanical, electrical and physical properties and low weight. One approach to access to these aims simultaneously is to use CNTRC plate with hole. Plate with various shape openings are applied as structural members to further reduce the weight of structures. Buckling and post-buckling behavior of plate subjected to in-plane loadings is so important to design and development of high performance structural components for stability (buckling and post-buckling).

Buckling and post buckling of nano plates have been studied by many researchers so far. Tounsi *et al*. (2013) presented the nonlocal effects on thermal buckling properties of double-walled carbon nanotubes. They show that the effect of shear deformation and rotary inertia on the buckling temperature is so apparent for the higher-order modes. The influence of surface energy on the post-buckling behavior of nanoplates was studied by Wang and Wang (2013). They showed that the influence of surface energy on the post-buckling load of the nanoplates becomes increasingly significant when the thickness of the plate decreases. Nonlocal post-buckling behavior of both uni-axially and bi-axially loaded graphene sheets in a polymer environment according to an orthotropic nano-plate model was proposed by Naderi and Saidi (2014). Chemi *et al*. (2015) presented Critical buckling load of chiral double-walled carbon nanotube using non-local theory elasticity. Sahmani *et al*. (2016) considered size-dependent axial buckling and post-buckling characteristics of cylindrical nanoshells in different temperatures. Baseri *et al*. (2016) investigated analytical solution for buckling of embedded laminated plates based on higher order shear deformation plate theory. Buckling of a single-layered graphene sheet embedded in visco-Pasternak medium via nonlocal first-order theory introduced by Zenkour (2016). Elmerabet *et al*. (2017a) investigated buckling temperature of a single-walled boron nitride nanotubes using a novel nonlocal beam model. Wu *et al*. (2017) analyzed thermal buckling and post-buckling of FG graphene nanocomposite plates. The post-buckling response of FG nanoplates by using the nonlocal elasticity theory of Eringen to consider the size effect was studied by Thai *et al*. (2018). They considered the influences of gradient index, nonlocal effect, ratio of compressive loads, boundary condition, thickness ratio and aspect ratio on the postbuckling behaviour of FG nanoplates.

*Corresponding author, Ph.D., Professor,
E-mail: rezakolahchi@duytan.edu.vn

ISSN: 2287-237X (Print), 2287-2388 (Online)

The famous classical plate theory (CLPT) which is based on Kirchhoff's hypothesis, supposes that straight lines normal to the mid-plane will be straight and normal to the mid-plane and will not change according to thickness stretching. CLPT cannot be applied in thick plates wherein shear deformation effects are more important because the transverse shear deformation is ignored in this theory. The FSDT is an improvement over the CLPT because in this theory transverse shear deformation is considered. In this theory, the transverse shear strain is presumed to be constant across the thickness; therefore, shear correction factor to correct the strain energy of shear deformation is required (Ghugal and Sayyad 2010). Size dependent bending and vibration analysis of FG micro beams based on modified couple stress theory and neutral surface position was analyzed by Al- Basyouni (Al-Basyouni *et al*. 2015). Liu *et al*. (2016) investigated the buckling and post-buckling behaviors of piezoelectric nanoplate based on the nonlocal Mindlin plate model and von Karman geometric nonlinearity. Soleimani *et al*. (2017) attempted to investigate the nonlocal post-buckling analysis of graphene sheets with initial imperfection based on FSDT. The effect of various parameters such as nonlocal parameter, edge length, boundary conditions, compression ratio, and aspect ratio on the post-buckling was studied. The results of this work represented the high accuracy of FSDT for post-buckling behavior of graphene sheets. A novel and simple higher order shear deformation theory for stability and vibration of FG sandwich plate was expressed by Sekkal *et al*. (2017). Youcef *et al*. (2018) discussed dynamic analysis of nanoscale beams including surface stress effects. Attia *et al*. (2018) presented a refined four variable plate theory for thermoelastic analysis of FGM plates resting on variable elastic foundations.

Recently, many works have been done to investigate the mechanical properties of FG-CNTRC micro plate. Shen and Zhang (2010) studied thermal buckling and post-buckling behavior of FG-CNTRC plates. The results demonstrate that the thermal post-buckling strength of the plate can be improved as a result of a FG reinforcement. In this paper, the Eshelby–Mori–Tanaka approach and the extended rule of mixture were applied in order to consider the effective material properties. Liew *et al*. (2014) carried out the post-buckling of FG-CNTRC cylindrical panels under axial compression using a meshless approach. Nonlinear post-buckling and vibration response of smart two-phase nanocomposite plates with surface-bonded piezoelectric layers under a combined mechanical, thermal and electrical loading was analyzed by Rafiee *et al*. (2015). Bending, buckling and vibration responses of FG-CNT beams were introduced by Tagrara *et al*. (2015). Jamali *et al*. (2016) presented buckling analysis of FG-CNTRC cut out plate using domain decomposition method and orthogonal polynomials. Agglomeration effects on the dynamic buckling of viscoelastic microplates reinforced with SWCNTs using Bolotin method was analyzed by Kolahchi and Cheraghbak (2017). In this research, agglomeration effects are considered based on Mori–Tanaka approach and dynamic instability region of structure is calculated based on Navier and Bolotin's methods.

There are some approaches in order to improve the mechanical behavior of system. In this research two parameters such as magnetic field and elastic medium are investigated. Mohammadi *et al*. (2014) studied the post-buckling instability of nonlinear nanobeam with geometric imperfection embedded in elastic foundation. They demonstrated that the bifurcation diagram of a curved nanobeam with initial sinusoidal configuration is sane as that of a straight nanobeam in its nearest buckling mode. Analytical modeling of wave propagation in viscoelastic CNTRC piezoelectric microplate surrounded by elastic medium was carried out by Ghorbanpour *et al*. (2015). Ebrahimi and Barati (2016) introduced analytical solution for nonlocal buckling characteristics of higher-order inhomogeneous nanosize beams embedded in elastic medium. Golmakani and Vahabi (2017) considered the nonlocal buckling analysis of FG annular nanoplates in an elastic medium with various boundary conditions. Tung (Tung 2017) studied the thermal buckling and post-buckling behavior of FG-CNTRC plates resting on elastic foundations with tangential-edge restraints. Ebrahimi and Barati (2016a) investigated an exact solution for buckling analysis of embedded piezo- electro-magnetically actuated nanoscale beams. Jamali *et al*. (2017) presented the wave propagation behavior of coupled viscoelastic FG-CNTRPC micro plates subjected to electro-magnetic fields surrounded by orthotropic visco-Pasternak foundation. Size dependent buckling and post-buckling analyses of FSDT magneto-electro-thermo elastic nanoplates based on nonlocal elasticity theory was analyzed by Ansari and Gholami (2016). Effects of triaxial magnetic field on the anisotropic nanoplates was presented by Karami *et al*. (2017).

According to aforementioned literature, there is not any paper which is about the effect of cut out on the post-buckling behavior of FG-CNTRC micro plate surrounded by elastic foundation under magnetic field. In order to investigate the behavior of plate, the FSDT is considered. CNTs are used to reinforce the plate through thickness in four different types such as $FG-X, FG-UD, FG-A$and $FG-O$. The structure is embedded in Pasternak medium and subjected to magnetic field. Based on domain decomposition and Rayleigh-Ritz methods in conjunction with Newton-Raphson iterative technique the post-buckling response of the system is obtained. The influence of some important parameters such as small scale effect, cut out dimension, different types of FG distributions of CNTs, volume fraction of CNTs, aspect ratio of plate, magnitude of magnetic field, elastic medium and biaxial load on the post-buckling behavior of system are calculated.

2. Description of system formulation

Fig. 1 demonstrates a FG-CNTRC micro rectangular cut out plate subjected to biaxial load and magnetic field embedded in elastic medium with geometrical characteristics as length a, width b and thickness h. Different distributions of CNTs through thickness such as $FG-X, FG-UD, FG-A$and $FG-O$ are assumed.

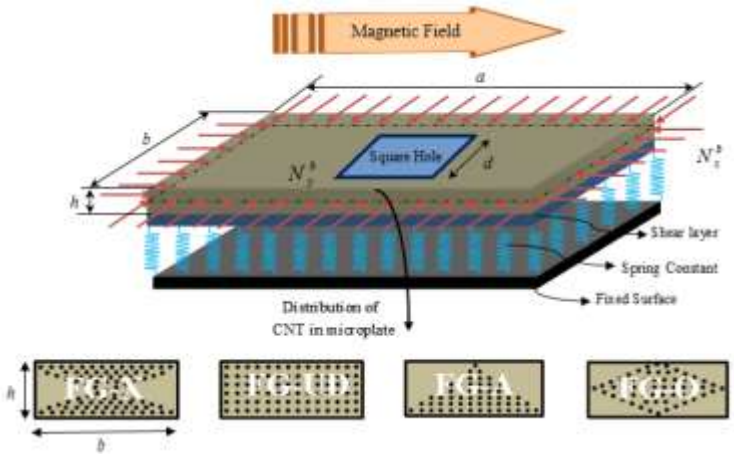

Fig. 1 A schematic of a FG-CNTRC micro cut out plate with four different CNTs distribution surrounded with elastic foundation subjected to biaxial loading and magnetic field

2.1 FSDT of plate

The displacement field based on Mindlin plate theory is explained as follows

$$u(x,y,z) = u_0(x,y) + z\phi_1(x,y), \tag{1a}$$

$$v(x,y,z) = v_0(x,y) + z\phi_2(x,y), \tag{1b}$$

$$w(\mathrm{x,y,z}) = \mathrm{w_0(x,y)}, \tag{1c}$$

Where u_0, v_0 and w_0 are in-plane displacements of the mid-plane in *x*, *y* and *z* directions, respectively. ϕ_1 and ϕ_2 are the rotations about *x* and *y* directions, respectively.

2.2 Material properties via extended rule of mixture

The micro composite plate in this study is composed of CNTs (for four different types such as FG-UD, FG-X, FG-A and FG-O) and matrix. In order to define mechanical properties of this combination, rule of mixture is employed as (Ghorbanpour Arani *et al*. 2016b)

$$E_{11} = \eta_1 V_{CNT} E_{11}^{CNT} + V_m E^m, \tag{2}$$

$$\frac{\eta_2}{E_{22}} = \frac{V_{CNT}}{E_{22}^{CNT}} + \frac{V_m}{E^m}, \tag{3}$$

$$\frac{\eta_3}{G_{12}} = \frac{V_{CNT}}{G_{12}^{CNT}} + \frac{V_m}{G^m}, \tag{4}$$

$$V_{CNT} + V_m = 1. \tag{5}$$

in which E^m, G^m are the properties of matrix and E_{11}^{CNT}, E_{22}^{CNT} and G_{12}^{CNT} show Young's moduli and shear modulus related to CNTs, respectively. The CNTs efficiency parameter,$\eta_j (j = 1,2,3)$, expose the scale-dependent material properties defined by matching the effective mechanical properties of CNTRC. V_{CNT} and V_m demonstrate volume fractions of CNT and matrix, respectively.

In this section different 4 types of laying up CNTs through thickness such as FG-UD, FG-X, FG-A and FG-O are considered as Fig. 1.

$$V_{CNT} = V_{CNT}^*, \qquad (UD) \tag{6}$$

$$V_{CNT} = \left(1 - \frac{2z}{h}\right) V_{CNT}^*, \qquad (FG-A) \tag{7}$$

$$V_{CNT} = 2\left(1 - \frac{2|z|}{h}\right) V_{CNT}^*, \qquad (FG-O) \tag{8}$$

$$V_{CNT} = 2\left(\frac{2|z|}{h}\right) V_{CNT}^*, \qquad (FG-X) \tag{9}$$

in which

$$V_{CNT}^* = \frac{W_{CNT}}{W_{CNT} + \left(\frac{\rho_{CNT}}{\rho_m}\right) - \left(\frac{\rho_{CNT}}{\rho_m}\right) W_{CNT}}, \tag{10}$$

w_{CNT} expresses the mass fraction of nanotube, ρ_{CNT} and $\rho_m$define the density of carbon nanotube and matrix, respectively. The Poisson's ratio, υ_{12} and density, ρ of micro composite plate are

$$\upsilon_{12} = V_{CNT}\upsilon_{12}^{CNT} + V_m \upsilon^m, \tag{11}$$

$$\rho = V_{CNT}\rho^{CNT} + V_m \rho^m, \tag{12}$$

where υ_{12}^{CNT} and υ^mdemonstrate Poisson's ratios of CNT and matrix, respectively.

2.3 Energy of system

Strain energy of micro composite plate may be calculated as

$$U = \frac{1}{2}\int_A \int_{\frac{-h}{2}}^{\frac{h}{2}} \left(\sigma_{xx}\varepsilon_{xx} + \sigma_{yy}\varepsilon_{yy} + \sigma_{yz}\gamma_{yz} + \sigma_{xz}\gamma_{xz} + \sigma_{xy}\gamma_{xy}\right) dz dA. \tag{13}$$

According to the Eringen's nonlocal elasticity theory (Eringen 2002), the constitutive equations of system is related to small scale effect and atomic forces. Local and nonlocal stresses, which are defined from the nonlocal balance law, may be extracted as (Ghorbanpour Arani *et al*. 2016a)

$$(1-\mu^2\nabla^2)\sigma_{ij}^{nl}=\sigma_{ij}^{l}=C:\varepsilon_{ij},\mu=e_0a, \tag{14}$$

where ∇^2 is the Laplace operation in the *x-y* coordinate system; σ_{ij}^{l} and σ_{ij}^{nl} express stress in local and nonlocal theories, respectively; a defines internal characteristic length, and e_0 is material constant extracted by the experiment.

Employing Eq. (14), the plane stress constitutive relation for a nonlocal FG-CNTRC micro plate is obtained as

$$\begin{Bmatrix}\sigma_{xx}^{nl}\\ \sigma_{yy}^{nl}\\ \sigma_{yz}^{nl}\\ \sigma_{xz}^{nl}\\ \sigma_{xy}^{nl}\end{Bmatrix}-\mu^2\nabla^2\begin{Bmatrix}\sigma_{xx}^{nl}\\ \sigma_{yy}^{nl}\\ \sigma_{yz}^{nl}\\ \sigma_{xz}^{nl}\\ \sigma_{xy}^{nl}\end{Bmatrix}=\begin{bmatrix}Q_{11} & Q_{12} & 0 & 0 & 0\\ & Q_{22} & 0 & 0 & 0\\ & & Q_{44} & 0 & 0\\ & & & Q_{55} & 0\\ sym. & & & & Q_{66}\end{bmatrix}\begin{Bmatrix}\varepsilon_{xx}\\ \varepsilon_{yy}\\ \gamma_{yz}\\ \gamma_{xz}\\ \gamma_{xy}\end{Bmatrix}, \tag{15}$$

$Q_{ij}(i,j=1,2,\ldots,6)$ is defined as

$$\begin{aligned}&Q_{11}=\frac{E_{11}}{1-\upsilon_{12}\upsilon_{21}},\quad Q_{22}=\frac{E_{22}}{1-\upsilon_{12}\upsilon_{21}},\\ &Q_{12}=\frac{\upsilon_{21}E_{11}}{1-\upsilon_{12}\upsilon_{21}},\\ &Q_{44}=G_{23},\quad Q_{55}=G_{13},\quad Q_{66}=G_{12}.\end{aligned} \tag{16}$$

The strain field extracted by applying strain-displacement relations in conjunction with von-Karman as

$$\begin{Bmatrix}\varepsilon_{xx}\\ \varepsilon_{yy}\\ \gamma_{yz}\\ \gamma_{xz}\\ \gamma_{xy}\end{Bmatrix}=\begin{Bmatrix}\varepsilon_{xx}^{0}\\ \varepsilon_{yy}^{0}\\ \gamma_{yz}^{0}\\ \gamma_{xz}^{0}\\ \gamma_{xy}^{0}\end{Bmatrix}+z\begin{Bmatrix}\varepsilon_{xx}^{1}\\ \varepsilon_{yy}^{1}\\ \gamma_{yz}^{1}\\ \gamma_{xz}^{1}\\ \gamma_{xy}^{1}\end{Bmatrix}, \tag{17}$$

in which

$$\begin{Bmatrix}\varepsilon_{xx}^{0}\\ \varepsilon_{yy}^{0}\\ \gamma_{yz}^{0}\\ \gamma_{xz}^{0}\\ \gamma_{xy}^{0}\end{Bmatrix}=\begin{Bmatrix}\dfrac{\partial u_0}{\partial x}+\dfrac{1}{2}\left(\dfrac{\partial w_0}{\partial x}\right)^2\\ \dfrac{\partial v_0}{\partial y}+\dfrac{1}{2}\left(\dfrac{\partial w_0}{\partial y}\right)^2\\ \dfrac{\partial w_0}{\partial y}+\phi_2\\ \dfrac{\partial w_0}{\partial x}+\phi_1\\ \dfrac{\partial u_0}{\partial y}+\dfrac{\partial v_0}{\partial x}+\dfrac{\partial w_0}{\partial x}\dfrac{\partial w_0}{\partial y}\end{Bmatrix}, \tag{18}$$

$$\begin{Bmatrix}\varepsilon_{xx}^{1}\\ \varepsilon_{yy}^{1}\\ \gamma_{yz}^{1}\\ \gamma_{xz}^{1}\\ \gamma_{xy}^{1}\end{Bmatrix}=\begin{Bmatrix}\dfrac{\partial\phi_1}{\partial x}\\ \dfrac{\partial\phi_2}{\partial y}\\ 0\\ 0\\ \dfrac{\partial\phi_1}{\partial x}+\dfrac{\partial\phi_2}{\partial y}\end{Bmatrix}. \tag{19}$$

The stress resultants N_{ij}^{nl}, M_{ij}^{nl} and Q_k^{nl} are expressed as

$$\begin{Bmatrix}N_{xx}^{nl}\\ N_{yy}^{nl}\\ N_{xy}^{nl}\end{Bmatrix}=\int_{-\frac{h}{2}}^{\frac{h}{2}}\begin{Bmatrix}\sigma_{xx}^{nl}\\ \sigma_{yy}^{nl}\\ \sigma_{xy}^{nl}\end{Bmatrix}dz, \tag{20}$$

$$\begin{Bmatrix}M_{xx}^{nl}\\ M_{yy}^{nl}\\ M_{xy}^{nl}\end{Bmatrix}=\int_{-\frac{h}{2}}^{\frac{h}{2}}z\begin{Bmatrix}\sigma_{xx}^{nl}\\ \sigma_{yy}^{nl}\\ \sigma_{xy}^{nl}\end{Bmatrix}dz, \tag{21}$$

$$\begin{Bmatrix}Q_y^{nl}\\ Q_x^{nl}\end{Bmatrix}=\kappa_s\int_{-\frac{h}{2}}^{\frac{h}{2}}\begin{Bmatrix}\sigma_{yz}^{nl}\\ \sigma_{xz}^{nl}\end{Bmatrix}dz, \tag{22}$$

k_s demonstrates the transverse shear correction coefficient. By using Eq. (15) with Eqs. (20)-(22), the nonlocal constitutive relations can be defined as

$$\begin{aligned}&(1-\mu^2\nabla^2)N_{xx}^{nl}\\ &=N_{xx}=A_{11}\frac{\partial u_0}{\partial x}+B_{11}\frac{\partial\phi_1}{\partial x}+\frac{1}{2}A_{11}\left(\frac{\partial w_0}{\partial x}\right)^2\\ &+A_{12}\frac{\partial v_0}{\partial y}+B_{12}\frac{\partial\phi_2}{\partial y}+\frac{1}{2}A_{12}\left(\frac{\partial w_0}{\partial y}\right)^2,\end{aligned} \tag{23}$$

$$\begin{aligned}&(1-\mu^2\nabla^2)N_{yy}^{nl}=N_{yy}\\ &=A_{12}\frac{\partial u_0}{\partial x}+B_{12}\frac{\partial\phi_1}{\partial x}+\frac{1}{2}A_{12}\left(\frac{\partial w_0}{\partial x}\right)^2\\ &+A_{22}\frac{\partial v_0}{\partial y}+B_{22}\frac{\partial\phi_2}{\partial y}+\frac{1}{2}A_{22}\left(\frac{\partial w_0}{\partial y}\right)^2,\end{aligned} \tag{24}$$

$$\begin{aligned}&(1-\mu^2\nabla^2)N_{xy}^{nl}=N_{xy}\\ &=A_{66}\frac{\partial}{\partial x}v_0+B_{66}\frac{\partial}{\partial x}\phi_2+A_{66}\frac{\partial}{\partial y}u_0\\ &+B_{66}\frac{\partial}{\partial y}\phi_1+A_{66}\left(\frac{\partial}{\partial x}w_0\right)\left(\frac{\partial}{\partial y}w_0\right),\end{aligned} \tag{25}$$

$$\begin{aligned}&(1-\mu^2\nabla^2)M_{xx}^{nl}=M_{xx}\\ &=B_{11}\frac{\partial}{\partial x}u_0+D_{11}\frac{\partial}{\partial x}\phi_1+0.5B_{11}\left(\frac{\partial}{\partial x}w_0\right)^2\\ &+B_{12}\frac{\partial}{\partial y}v_0+D_{12}\frac{\partial}{\partial y}\phi_2+0.5B_{12}\left(\frac{\partial}{\partial y}w_0\right)^2,\end{aligned} \tag{26}$$

$$\begin{aligned}&(1-\mu^2\nabla^2)M_{yy}^{nl}=M_{yy}\\ &=B_{12}\frac{\partial}{\partial x}u_0+D_{12}\frac{\partial}{\partial x}\phi_1+0.5B_{12}\left(\frac{\partial}{\partial x}w_0\right)^2\\ &+B_{22}\frac{\partial}{\partial y}v_0+D_{22}\frac{\partial}{\partial y}\phi_2+0.5B_{22}\left(\frac{\partial}{\partial y}w_0\right)^2,\end{aligned} \tag{27}$$

$$(1-\mu^2\nabla^2)M_{xy}^{nl} = M_{xy} = B_{66}\frac{\partial}{\partial x}v_0 + D_{66}\frac{\partial}{\partial x}\phi_2 + B_{66}\frac{\partial}{\partial y}u_0 + D_{66}\frac{\partial}{\partial y}\phi_1 + B_{66}\left(\frac{\partial}{\partial x}w_0\right)\left(\frac{\partial}{\partial y}w_0\right), \quad (28)$$

$$(1-\mu^2\nabla^2)Q_{xz}^{nl} = Q_{xz} = \kappa_s A_{55}\frac{\partial}{\partial x}w_0 + \kappa_s A_{55}\phi_1, \quad (29)$$

$$(1-\mu^2\nabla^2)Q_{yz}^{nl} = Q_{yz} = \kappa_s A_{44}\frac{\partial}{\partial y}w_0 + \kappa_s A_{44}\phi_2. \quad (30)$$

the stiffness components may be extracted as

$$(A_{ij}, B_{ij}, D_{ij}) = \int_{-\frac{h}{2}}^{\frac{h}{2}} Q_{ij}(z)\,(1, z, z^2)dz. \quad (31)$$

Therefore

$$\begin{aligned} U = \frac{1}{2}\int_A \Bigg(& N_{xx}\left(\frac{\partial}{\partial x}u_0 + 0.5\left(\frac{\partial}{\partial x}w_0\right)^2\right) \\ & + M_{yy}\frac{\partial}{\partial y}\phi_2 + N_{yy}\left(\frac{\partial}{\partial y}v_0 + 0.5\left(\frac{\partial}{\partial y}w_0\right)^2\right) \\ & + M_{xx}\frac{\partial}{\partial x}\phi_1 + N_{xy}\left(\frac{\partial u_0}{\partial y} + \frac{\partial v_0}{\partial x} + \left(\frac{\partial w_0}{\partial x}\right)\left(\frac{\partial w_0}{\partial y}\right)\right) \\ & + Q_x\left(\frac{\partial}{\partial x}w_0 + \phi_1\right) + M_{xy}\left(\frac{\partial}{\partial y}\phi_1 + \frac{\partial}{\partial x}\phi_2\right) \\ & + Q_y\left(\frac{\partial}{\partial y}w_0 + \phi_2\right)\Bigg) dA. \end{aligned} \quad (32)$$

Extended formulation of strain energy is presented in Appendix A.

The FG-CNTRC micro plate is exposed to three types of external forces such as biaxial compression load, elastic medium and magnetic field.

According to Fig. 1, micro plate is subjected to biaxial loading ($N_x^b = -F$and $N_y^b = -kF$); therefore, the work of compression load is calculated as

$$W_b = -\frac{1}{2}\int_A \left(N_x^b\left(\frac{\partial}{\partial x}w(x,y)\right)^2 + N_y^b\left(\frac{\partial}{\partial y}w(x,y)\right)^2\right) dA. \quad (33)$$

Nonlocal extended formulation of is existed in Appendix A.

The micro plate is surrounded by elastic medium; subsequently, the work of medium is

$$W_f = -\int_A \left(K_w w - G_p\nabla^2 w\right) w\, dA, \quad (34)$$

K_w and G_p represent Winkler's spring modulus and shear foundation parameter, respectively. Nonlocal extended formulation of w_f is demonstrated in Appendix A.

Based on Fig. 1 the system is subjected to longitudinal magnetic field, $\overrightarrow{H_0} = (H_x, 0, 0)$, thus the Maxwell's relations can be expressed as

$$\overrightarrow{f_m} = \eta\left(\nabla\times\left(\nabla\times\left(\vec{u}\times\overrightarrow{H_0}\right)\right)\right)\times\overrightarrow{H_0}, \quad (35)$$

where $\vec{u}$ is displacement vector, η shows the magnetic permeability of plate and ∇ represents the gradient operator. The components of the Lorentz force per unit volume of the micro composite plate are calculated as

$$f_{mx} = 0, \quad (36)$$

$$f_{my} = \eta {H_x}^2\left(\frac{\partial^2}{\partial x^2}v_0\right) + \eta {H_x}^2 z\left(\frac{\partial^2}{\partial x^2}\phi_2\right) + \eta {H_x}^2\left(\frac{\partial^2}{\partial y^2}v_0\right) + \eta {H_x}^2 z\left(\frac{\partial^2}{\partial y^2}\phi_2\right), \quad (37)$$

$$f_{mz} = \eta {H_x}^2\left(\frac{\partial}{\partial y}\phi_2\right) + \eta {H_x}^2\left(\frac{\partial^2}{\partial x^2}w_0\right). \quad (38)$$

The generated forces ($F_m = \int_{-h/2}^{h/2} f_m dz$) and the bending moment ($M_m = \int_{-h/2}^{h/2} z f_m dz$) may be expressed as

$$F_{mx} = 0, \quad (39)$$

$$F_{my} = \eta {H_x}^2\left(\frac{\partial^2}{\partial x^2}v_0\right)h + \eta {H_x}^2\left(\frac{\partial^2}{\partial y^2}v_0\right)h, \quad (40)$$

$$F_{mz} = \eta {H_x}^2\left(\frac{\partial}{\partial y}\phi_2\right)h + \eta {H_x}^2\left(\frac{\partial^2}{\partial x^2}w_0\right)h, \quad (41)$$

$$M_{mx} = 0, \quad (42)$$

$$M_{my} = \frac{1}{12}\left(\left(\frac{\partial^2}{\partial x^2}\phi_2\right)\eta {H_x}^2 + \left(\frac{\partial^2}{\partial y^2}\phi_2\right)\eta {H_x}^2\right)h^3. \quad (43)$$

Finally, Lorentz work can be defined as

$$W_m = \int_A \left(F_{mx}u + F_{my}v + F_{mz}w + \left(M_{mx,x} + M_{my,y}\right)w\right)dA. \quad (44)$$

Nonlocal extended formulation of w_m is presented in Appendix A.

Eventually, total energy of FG-CNTRC micro plate is defined as

$$\begin{aligned} \Pi = U - W = \int_A \Bigg\{ \frac{1}{2}\Bigg[& N_{xx}\left(\frac{\partial}{\partial x}u_0 + 0.5\left(\frac{\partial}{\partial x}w_0\right)^2\right) \\ & + N_{yy}\left(\frac{\partial}{\partial y}v_0 + 0.5\left(\frac{\partial}{\partial y}w_0\right)^2\right) + M_{xx}\frac{\partial}{\partial x}\phi \\ & + N_{xy}\left(\frac{\partial u_0}{\partial y} + \frac{\partial v_0}{\partial x} + \left(\frac{\partial w_0}{\partial x}\right)\left(\frac{\partial w_0}{\partial y}\right)\right)_1 \end{aligned} \quad (45)$$

$$+M_{yy}\frac{\partial}{\partial y}\phi_2 + M_{xy}\left(\frac{\partial\phi_1}{\partial y}+\frac{\partial\phi_2}{\partial x}\right)$$
$$+Q_x\left(\frac{\partial w_0}{\partial x}+\phi_1\right)+Q_y\left(\frac{\partial w_0}{\partial y}+\phi_2\right)\Big]$$
$$-\frac{1}{2}(1-\mu^2\nabla^2)\left[N_x^b\left(\frac{\partial}{\partial x}w\right)^2+N_y^b\left(\frac{\partial}{\partial y}w\right)^2\right] \quad (45)$$
$$-(1-\mu^2\nabla^2)\big[(K_w w-G_p\nabla^2 w)w\big]$$
$$+(1-\mu^2\nabla^2)\big[F_{mx}u+F_{my}v+F_{mz}w$$
$$+\big(Mmy,y_{mx,x}w\big]\big)dA.\}$$

3. Post-buckling analysis of cut out FG-CNTRC micro plate

The displacement values based on the simply supported rectangular plate can be expressed as

$$w_0(x,y)=w_{mn}\,sin\left(\frac{m\pi x}{a}\right)sin\left(\frac{n\pi y}{b}\right), \quad (46)$$

$$\phi_1(x,y)=\phi_{1mn}\,cos\left(\frac{m\pi x}{a}\right)sin\left(\frac{n\pi y}{b}\right), \quad (47)$$

$$\phi_2(x,y)=\phi_{2mn}\,sin\left(\frac{m\pi x}{a}\right)cos\left(\frac{n\pi y}{b}\right), \quad (48)$$

in which m and n show mode numbers and $\{w_{mn},\phi_{1mn},\phi_{2mn}\}$ are amplitudes. By substituting Eqs. (46)-(48) to Eq. (45), the following matrix form is extracted

$$(K_L+K_{NL}-FK_G)d=0, \quad (49)$$

where K_L, K_{NL} and K_G represent linear, nonlinear and geometric stiffness matrix, respectively. F is the post bucking load and d is equal to $\{w_{mn},\phi_{1mn},\phi_{2mn}\}^T$.

Eq. (49) can be simplified to linear static buckling formulation of FG-CNTRC micro plate by ignoring nonlinear stiffness matrix such as follow

$$(K_L-F_{cr}K_G)d=0, \quad (50)$$

in which F_{cr} represents the critical buckling load calculated through Rayleigh-Ritz method.

The post-buckling response of the micro plate can be obtained by using Eq. (49) via Rayleigh-Ritz method and Newton-Raphson iterative technique. At the beginning, the iterative scheme starts by solving an eigenvalue problem of Eq. (50) with neglecting the geometric nonlinear matrix to calculate the eigenvalue and corresponding eigenvector such as the first guesses for the buckling load and mode shape. Afterwards, the post-buckling response of plate can be calculated by applying iterative process.

With respect to Fig. 1 it is understood that the rectangular plate in this study has central square cut out; therefore, in order to approximate the post-buckling behavior of system, firstly by using domain decomposition method (Lam *et al*. 1989, Liew *et al*. 1993, 2001, Liew *et al*. 2003, Pan *et al*. 2013) the FG-CNTRC micro plate divide to four sections such as Fig. 2. After that by using Eq. (45), energy equation of each area is calculated and

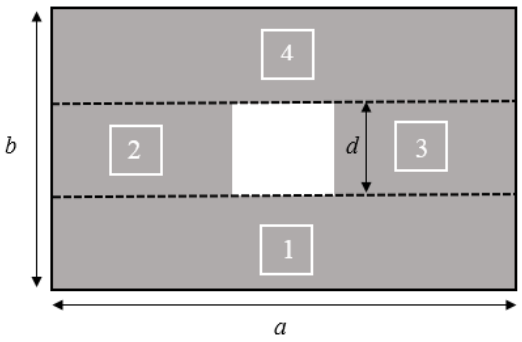

Fig. 2 Division of plate into four different areas

eventually energy equation of total plate is summation of four areas. Finally, post-buckling response of total plate is extracted by utilizing Eqs. (46)-(50) through Rayleigh-Ritz method and Newton-Raphson iterative technique.

4. Numerical results

The effect of cut out on post-buckling behavior of FG-CNTRC micro plate reinforced in four different types ($FG-X, FG-UD, FG-A$and $FG-O$) and embedded in elastic medium subjected to magneto-mechanical load is studied in this essay. The influence of some important parameters such as small scale effect, cut out dimension, different types of FG distributions of CNTs, volume fraction of CNTs, aspect ratio of plate, magnitude of magnetic field, elastic medium and biaxial load on the post-buckling behavior of system are presented.

To validate the results of this study with other papers, a comparison among the post-buckling analysis of this study and Wang and Wang (2013) is considered in Fig. 3. In this figure, post-buckling load in terms of maximum deflection is plotted. It is obvious that the present results closely match with those calculated by Wang and Wang (2013).

Fig. 4 indicates a comparison between the results of present article and ref. (Jafari *et al*. 2012). In this figure, buckling load in terms of dimension of plate is demonstrated. It is apparent that the present results closely

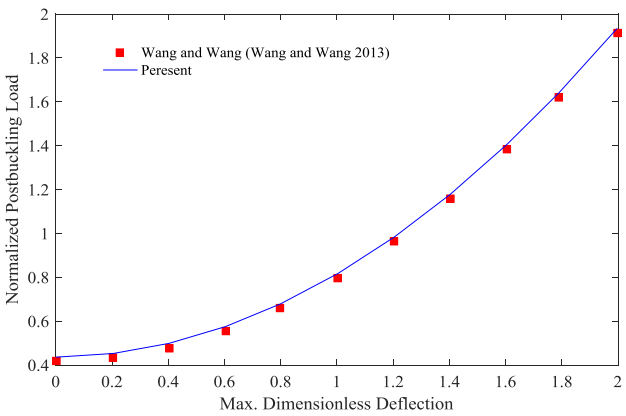

Fig. 3 Comparison of post-buckling load versus maximum deflection

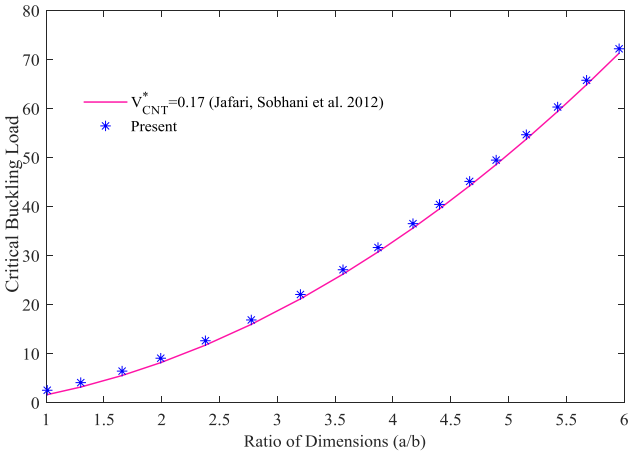

Fig. 4 Comparison of critical buckling load in the case of UD-CNTs distribution for various values of a/b

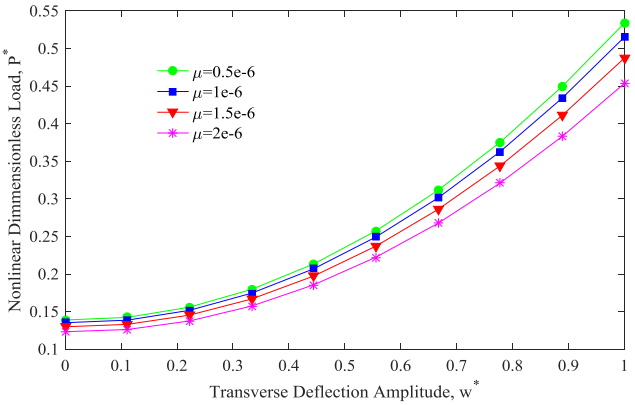

Fig. 5 Variation of dimensionless post-buckling load by considering dimensionless deflection amplitude for different nonlocal parameter

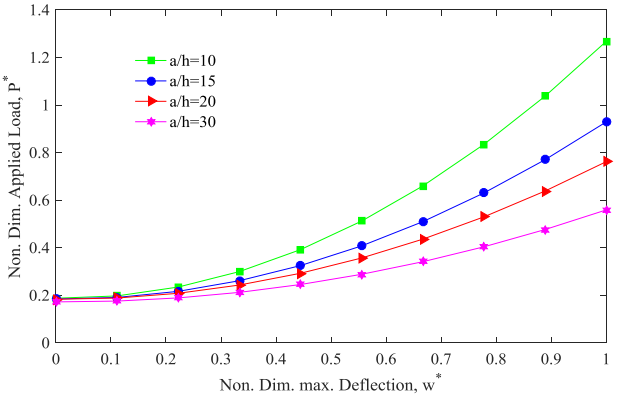

Fig. 6 Dimensionless post-buckling load versus dimensionless deflection amplitude for different aspect ratio

match with (Jafari *et al*. 2012).

Fig. 5 indicates that variations of the post-buckling load and deflection amplitude are a function of the nonlocal small scale. It in noticed that all the figures presented in this section are based on FG-UD. It can be understood that the

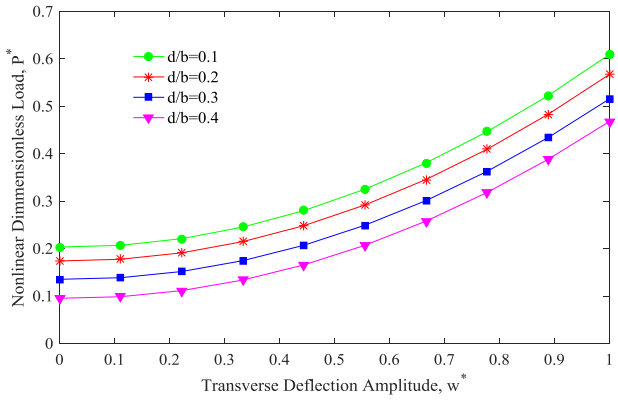

Fig. 7 Dimensionless post-buckling load versus dimensionless amplitude of deflection for different length of square cut out

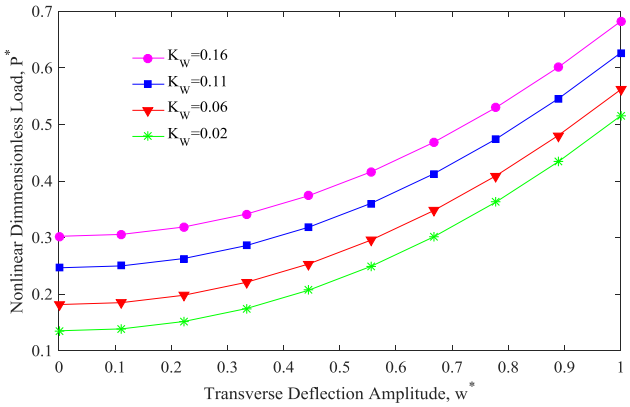

Fig. 8 Effect of the Winkler modulus parameter on the dimensionless post-buckling versus dimensionless deflection amplitude

dimensionless post-buckling load decreases with increasing nonlocal parameter. The reason is that the stiffness of the micro composite plate tends to decreases when the nonlocal parameter is considered, thus the post-buckling loads are reduced.

The effect of aspect ratio on dimensionless post-buckling load in terms of dimensionless amplitude of deflection is transparent in Fig. 6.

It is obvious by increasing length of plate, dimensionless post-buckling load decreases, it is due to the fact that by changing the length of plate to high number the stiffness of plate tend to reduce. Moreover, Fig. 7 shows the influence of magnitude of square cut out on the post-buckling load and deflection. The figure depicts that by increasing length of square stiffness of plate reduces; therefore, the post-buckling load decreases subsequently.

The effect of the elastic medium on post-buckling response is expressed in this section. Figs. 8 and 9 consider the influence of the elastic medium on post-buckling load based on different magnitude of dimensionless Winkler modulus parameter (K_W) and shear modulus parameter (G_P). It is apparent that Winkler modulus parameter and shear modulus parameter, improve the post-buckling behavior of micro plate, because considering elastic

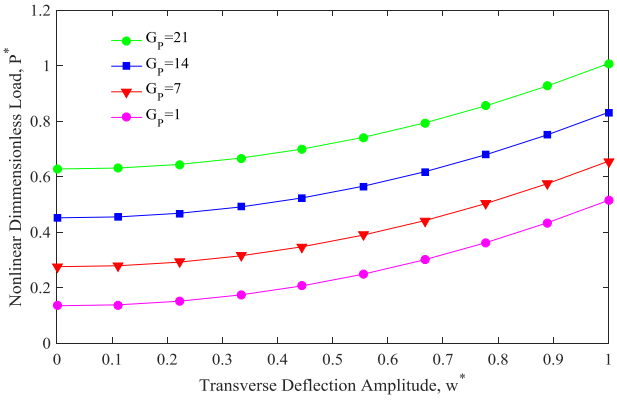

Fig. 9 Dimensionless post-buckling load versus dimensionless deflection amplitude for different shear modulus parameter

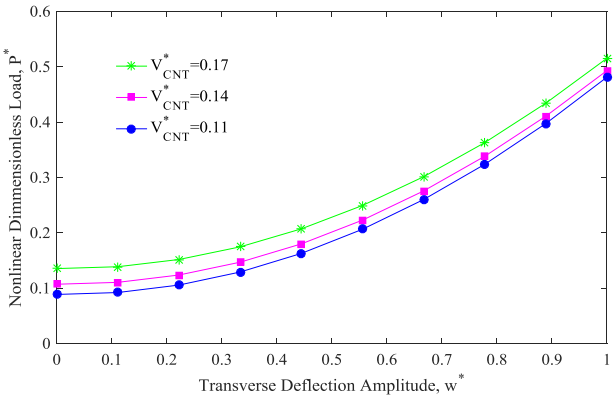

Fig. 11 Variation of dimensionless post-buckling load in terms of dimensionless deflection amplitude for different volume fraction

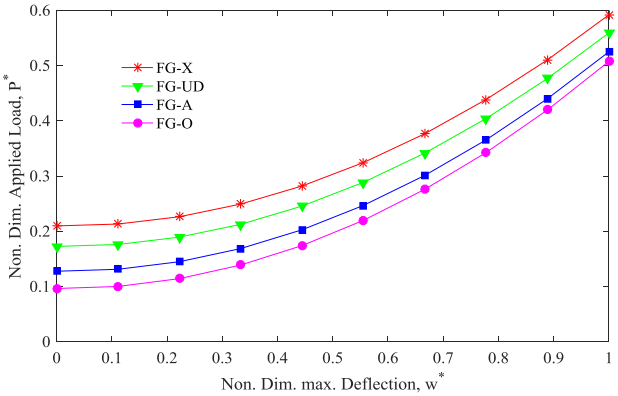

Fig. 10 Influence of the different distribution of CNTs on the dimensionless post-buckling load versus dimensionless deflection amplitude

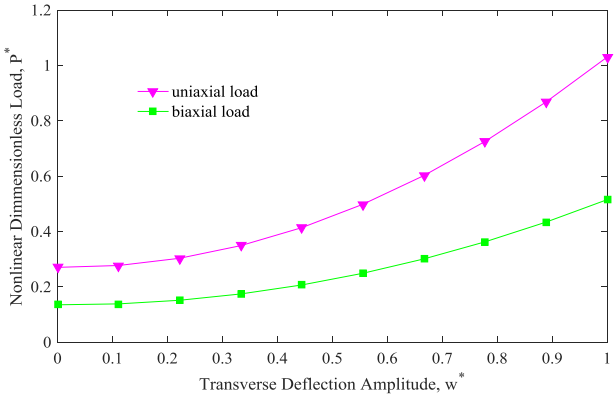

Fig. 12 Influence of biaxial and uniaxial compression load on the dimensionless post-buckling load versus dimensionless deflection amplitude

medium improves the stiffness of system and finally increases post-buckling load behavior. By analyzing the trend of Figs. 8 and 9, the influence of Pasternak foundation is more considerable than Winkler foundation.

The influence of four different kinds of FG distributions of CNTs on the post-buckling load is demonstrated in Fig. 10. It can be understood that the post-buckling response of $FG-X$ is more than other distributions.

The reason is that in the $FG-X$ distribution, CNTs have more distance from mid-plane and the stiffness of system is more than other FG types subsequently. Volume fraction of CNTs is one of the important factors of CNTRC plate; thus, variation of post-buckling versus deflection according to different volume fractions is examined in Fig. 11. It is concluded that increase volume fraction causes more post-buckling load, because volume fraction is a symbol of CNTs volume in composite structure; therefore, increase volume fraction improves mechanical properties of system.

Fig. 12 indicates the effect of considering biaxial and uniaxial loading on the post-buckling response of micro composite plate in terms of deflection. It is apparent that considering biaxial compression force reduces the post-buckling response of plate. It is due to the fact that by imposing biaxial load to the plate the intense of compression force is more than uniaxial load; therefore, the post-buckling behavior of system decreases.

The variation of dimensionless post-buckling load versus dimensionless deflection in terms of dimensionless magnetic field is plotted in Fig. 13. It can be seen magnetic field has positive effect on post-buckling load, because magnetic field imposes force to system, so system changes

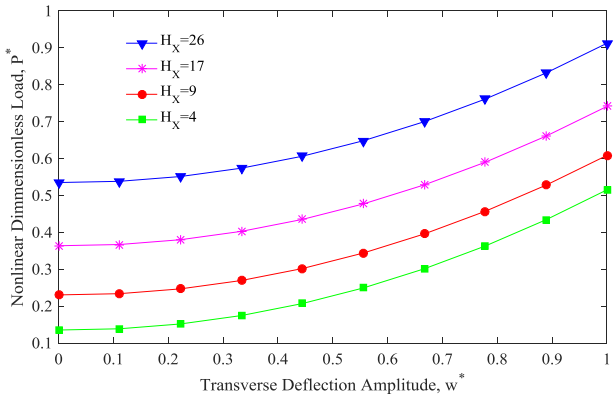

Fig. 13 Effect of magnetic field on the dimensionless post-buckling load versus dimensionless deflection amplitude

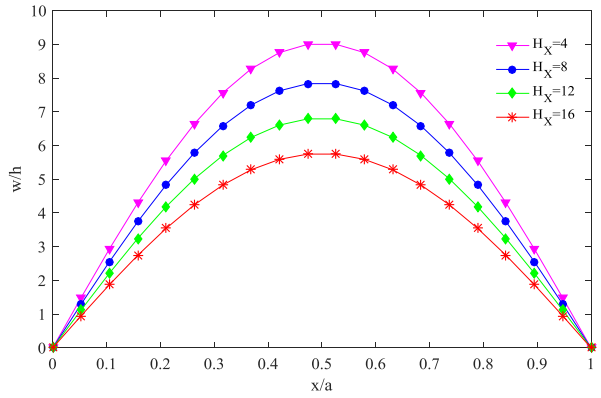

Fig. 14 Deflection of plate based on the simply support boundary condition in terms of magnetic field

to stiffer situation than previous. So, magnetic field can be applied as a controlling parameter to enhance the behavior of system.

Fig. 14 indicates that variations of the plate deflection are a function of magnetic field. It is noticed that this figure is presented based on FG-UD. It can be understood that the deflection of plate decreases with increasing magnetic field. The reason is that magnetic field has positive effect and imposes force to system, therefore, the deflection of plate decreases.

5. Conclusions

According to nonlocal elasticity theory, magneto-mechanical post-buckling response of FG-CNTRC micro plates with central opening was presented in this work. By use of FSDT and energy method, total energy of system was obtained and then nonlinear post-buckling of system was analyzed by use of analytical method. The effect of the magnetic field, functionally graded distributions of CNTs, volume fraction of CNTs, small scale parameter, aspect ratio, square cut out, biaxial compression load and elastic medium on the post-buckling behavior of the system were discussed in details. Results demonstrated that $FG-X$ and $FG-O$ distribution have maximum and minimum post-buckling load, respectively. Results demonstrated that:

- Post-buckling load decreases with increasing nonlocal parameter. Because, the stiffness of the micro composite plate tends to decreases when the nonlocal parameter is considered.
- By increasing dimensions of plate the post-buckling load of plate with square cut out decreases.
- By increasing the length of cut out in plate, the stiffness reduces; therefore, the post-buckling load decreases subsequently.
- Winkler modulus parameter and shear modulus parameter improve the post-buckling behavior of system, because considering elastic medium improves the stiffness of system.
- Increasing CNTs volume fraction causes more post-buckling load, because volume fraction is a symbol of CNTs volume in composite structure; therefore, increase volume fraction improves mechanical properties of system.
- The influence of four different kinds of FG distributions of CNTs on the post-buckling load was considered and it was apparent that the post-buckling response of $FG-X$ was more than other distributions.
- Considering biaxial compression force reduces the post-buckling response of plate. It is due to the fact that by imposing biaxial load to the plate the intense of compression force is more than uniaxial load.
- Magnetic field has positive effect on post-buckling load, because magnetic field imposes force to system, so system changes to stiffer situation than previous.

The results provided in this article would be useful in design and manufacturing of composite systems especially in nano/micro-mechanical systems.

References

Al-Basyouni, K.S., Tounsi, A. and Mahmoud, S.R. (2015), "Size dependent bending and vibration analysis of functionally graded micro beams based on modified couple stress theory and neutral surface position", *Compos. Struct.*, **125** 621-630. https://doi.org/10.1016/j.compstruct.2014.12.070

Ansari, R. and Gholami, R. (2016), "Size-dependent buckling and postbuckling analyses of first-order shear deformable magneto-electro-thermo elastic nanoplates based on the nonlocal elasticity theory", *Int. J. Struct. Stab. Dyn.*, **17**(1), 1750014. https://doi.org/10.1142/S0219455417500146

Attia, A., Anis Bousahla, A., Tounsi, A., Hassan, S. and Alwabli, A.S. (2018), "A refined four variable plate theory for thermoelastic analysis of FGM plates resting on variable elastic foundations", *Struct. Eng. Mech., Int. J.*, **65**(4), 453-464. https://doi.org/10.12989/sem.2018.65.4.453

Baseri, V., Soleimani Jafari, G. and Kolahchi, R. (2016), "Analytical solution for buckling of embedded laminated plates based on higher order shear deformation plate theory", *Steel Compos. Struct., Int. J.*, **21**(4), 883-919. https://doi.org/10.12989/scs.2016.21.4.883

Chemi, A., Heireche, H., Zidour, M., Kaddour, R. and Bousahla, A.A. (2015), "Critical buckling load of chiral double-walled carbon nanotube using non-local theory elasticity", *Adv. Nano Res., Int. J.*, **3**(4), 193-206. https://doi.org/10.12989/anr.2015.3.4.193

Ebrahimi, F. and Barati, M.R. (2016a), "Analytical solution for nonlocal buckling characteristics of higher-order inhomogeneous nanosize beams embedded in elastic medium", *Adv. Nano Res., Int. J.*, **4**(3), 229-249. https://doi.org/10.12989/anr.2016.4.3.229

Ebrahimi, F. and Barati, M.R. (2016b), "An exact solution for buckling analysis of embedded piezo- electro-magnetically actuated nanoscale beams", *Adv. Nano Res., Int. J.*, **4**(2), 65-84. https://doi.org/10.12989/anr.2016.4.2.065

Elmerabet, A.H., Heireche, H., Tounsi, A. and Semmah, A. (2017a), "Buckling temperature of a single-walled boron nitride nanotubes using a novel nonlocal beam model", *Adv. Nano Res., Int. J.*, **5**(1), 1-12. https://doi.org/10.12989/anr.2017.5.1.001

Elmerabet, A.H., Heireche, H., Tounsi, A. and Semmah, A. (2017b), "Buckling temperature of a single-walled carbon nanotube using nonlocal Timoshenko beam model", *J. Computat. Theor. Nanosci.*, **7**(11), 2367-2371.

https://doi.org/10.1166/jctn.2010.1621
Eringen, A.C. (2002), *Nonlocal Continuum Field Theories*, Springer Science and Business Media.
Ghorbanpour Arani, A., Jamali, M., Mosayyebi, M. and Kolahchi, R. (2015), "Analytical modeling of wave propagation in viscoelastic functionally graded carbon nanotubes reinforced piezoelectric microplate under electro-magnetic field", *Proceedings of the Institution of Mechanical Engineers, Part N: Journal of Nanoengineering and Nanosystems*, **231**(1), 17-33. https://doi.org/10.1177/0954406215627830
Ghorbanpour Arani, A., Jamali, M., Ghorbanpour-Arani, A.H., Kolahchi, R. and Mosayyebi, M. (2016a), "Electro-magneto wave propagation analysis of viscoelastic sandwich nanoplates considering surface effects", *Proceedings of the Institution of Mechanical Engineers, Part C: Journal of Mechanical Engineering Science*, **231**(2), 387-403. https://doi.org/10.1177/0954406215627830
Ghorbanpour Arani, A., Jamali, M., Mosayyebi, M. and Kolahchi, R. (2016b), "Wave propagation in FG-CNT-reinforced piezoelectric composite micro plates using viscoelastic quasi-3D sinusoidal shear deformation theory", *Compos. Part B*, **95**, 209-224. https://doi.org/10.1016/j.compositesb.2016.03.077
Ghugal, Y.M. and Sayyad, A.S. (2010), "A static flexure of thick isotropic plates using trigonometric shear deformation theory", *J. Solid Mech.*, **2**(1), 79-90.
Golmakani, M.E. and Vahabi, H. (2017), "Nonlocal buckling analysis of functionally graded annular nanoplates in an elastic medium with various boundary conditions", *Microsyst. Technol.* **23**(8), 3613-3628. https://doi.org/10.1007/s00542-016-3210-y
Jafari Mehrabadi, S., Sobhani Aragh, B., Khoshkhahesh, V. and Taherpour, A. (2012), "Mechanical buckling of nanocomposite rectangular plate reinforced by aligned and straight single-walled carbon nanotubes", *Compos. Part B*, **43**, 2031-2040. https://doi.org/10.1016/j.compositesb.2012.01.067
Jamali, M., Shojaee, T., Kolahchi, R. and Mohammadi, B. (2016), "Buckling analysis of nanocomposite cut out plate using domain decomposition method and orthogonal polynomials", *Steel Compos. Struct., Int. J.*, **22**(3), 691-712. https://doi.org/10.12989/scs.2016.22.3.691
Jamali, M., Arani, A.G., Mosayyebi, M., Kolahchi, R. and Esfahani, R.T. (2017), "Wave propagation behavior of coupled viscoelastic FG-CNTRPC micro plates subjected to electro-magnetic fields surrounded by orthotropic visco-Pasternak foundation", *Microsyst. Technol.*, **23**(8), 3791-3816. https://doi.org/10.1007/s00542-016-3232-5
Karami, B., Janghorban, M. and Tounsi, A. (2017), "Effects of triaxial magnetic field on the anisotropic nanoplates", *Steel Compos. Struct., Int. J.*, **25**(3), 361-374. https://doi.org/10.12989/scs.2017.25.3.361
Kolahchi, R. and Cheraghbak, A. (2017), "Agglomeration effects on the dynamic buckling of viscoelastic microplates reinforced with SWCNTs using Bolotin method", *Nonlinear Dyn.*, **90**(1), 479-492. https://doi.org/10.1007/s11071-017-3676-x
Lam, K.Y., Hung, K.C. and Chow, S.T. (1989), "Vibration analysis of plates with cutouts by the modified Rayleigh-Ritz method", *Appl. Acoust.*, **28**(1), 49-60. https://doi.org/10.1016/0003-682X(89)90030-3
Liew, K.M., Hung, K.C. and Lim, M.K. (1993), "Method of domain decomposition in vibrations of mixed edge anisotropic plates", *Int. J. Solids Struct.*, **30**(23), 3281-3301. https://doi.org/10.1016/0020-7683(93)90114-M
Liew, K.M., Ng, T.Y. and Kitipornchai, S. (2001), "A semi-analytical solution for vibration of rectangular plates with abrupt thickness variation", *Int. J. Solids Struct.*, **38**(28), 4937-4954. https://doi.org/10.1016/S0020-7683(00)00329-2
Liew, K.M., Kitipornchai, S., Leung, A.Y.T. and Lim, C.W. (2003), "Analysis of the free vibration of rectangular plates with central cut-outs using the discrete Ritz method", *Int. J. Mech. Sci.*, **45**(5), 941-959. https://doi.org/10.1016/S0020-7403(03)00109-7
Liew, K.M., Lei, Z.X., Yu, J.L. and Zhang, L.W. (2014), "Postbuckling of carbon nanotube-reinforced functionally graded cylindrical panels under axial compression using a meshless approach", *Comput. Methods Appl. Mech. Eng.*, **268**, 1-17. https://doi.org/10.1016/j.cma.2013.09.001
Liu, C., Ke, L.-L., Yang, J., Kitipornchai, S. and Wang, Y.-S. (2016), "Buckling and post-buckling analyses of size-dependent piezoelectric nanoplates", *Theor. Appl. Mech. Lett.*, **6**(6), 253-267. https://doi.org/10.1142/S0219455413500673
Mohammadi, H., Mahzoon, M., Mohammadi, M. and Mohammadi, M. (2014), "Postbuckling instability of nonlinear nanobeam with geometric imperfection embedded in elastic foundation", *Nonlinear Dyn.*, **76**(4), 2005-2016. https://doi.org/10.1007/s11071-014-1264-x
Naderi, A. and Saidi, A.R. (2014), "Nonlocal postbuckling analysis of graphene sheets in a nonlinear polymer medium", *Int. J. Eng. Sci.*, **81**, 49-65. https://doi.org/10.1016/j.ijengsci.2014.04.004
Pan, Z., Cheng, Y. and Liu, J. (2013), "A semi-analytical analysis of the elastic buckling of cracked thin plates under axial compression using actual non-uniform stress distribution", *Thin-Wall. Struct.*, **73**, 229-241. https://doi.org/10.1016/j.tws.2013.08.007
Rafiee, M., He, X.Q., Mareishi, S. and Liew, K.M. (2015), "Nonlinear response of piezoelectric nanocomposite plates: Large deflection, post-buckling and large amplitude vibration", *Int. J. Appl. Mech.*, **7**(5), 1550074. https://doi.org/10.1142/S175882511550074X
Sahmani, S., Aghdam, M.M. and Bahrami, M. (2016), "Size-dependent axial buckling and postbuckling characteristics of cylindrical nanoshells in different temperatures", *Int. J. Mech. Sci.*, **107**, 170-179. https://doi.org/10.1016/j.ijmecsci.2016.01.014
Sekkal, M., Fahsi, B., Tounsi, A. and Hassan, S. (2017), "A novel and simple higher order shear deformation theory for stability and vibration of functionally graded sandwich plate", *Steel Compos. Struct., Int. J.*, **25**(4), 389-401. https://doi.org/10.12989/scs.2017.25.4.389
Shen, H.-S. and Zhang, C.-L. (2010), "Thermal buckling and postbuckling behavior of functionally graded carbon nanotube-reinforced composite plates", *Mater. Des.*, **31**(7), 3403-3411. https://doi.org/10.1016/j.matdes.2010.01.048
Soleimani, A., Naei, M.H. and Mashhadi, M.M. (2017), "Nonlocal postbuckling analysis of graphene sheets with initial imperfection based on first order shear deformation theory", *Results Phys.*, **7**, 1299-1307. https://doi.org/10.1016/j.rinp.2017.03.003
Tagrara, S.H., Benachour, A., Bachir Bouiadjra, M. and Tounsi, A. (2015), "On bending, buckling and vibration responses of functionally graded carb on nanotube-reinforced composite beams", *Steel Compos. Struct., Int. J.*, **19**(5), 1259-1277. https://doi.org/10.12989/scs.2015.19.5.1259
Thai, S., Thai, H.-T., Vo, T.P. and Lee, S. (2018), "Postbuckling analysis of functionally graded nanoplates based on nonlocal theory and isogeometric analysis", *Compos. Struct.*, **201**, 13-20. https://doi.org/10.1016/j.compstruct.2018.05.116
Tounsi, A., Benguediab, S., Bedia, E.A.A., Semmah, A. and Zidour, M. (2013), "Nonlocal effects on thermal buckling properties of double-walled carbon nanotubes", *Adv. Nano Res., Int. J.*, **1**(1), 1-11. https://doi.org/10.12989/anr.2013.1.1.001
Tung, H.V. (2017), "Thermal buckling and postbuckling behavior of functionally graded carbon-nanotube-reinforced composite plates resting on elastic foundations with tangential-edge restraints", *J. Therm. Stresses*, **40**(5), 641-663.

https://doi.org/10.1080/01495739.2016.1254577
Wang, K.F. and Wang, B.L. (2013), "Effect of surface energy on the non-linear postbuckling behavior of nanoplates", *Int. J. Non-Linear Mech.*, **55**, 19-24. https://doi.org/10.1016/j.ijnonlinmec.2013.04.004
Wu, H., Kitipornchai, S. and Yang, J. (2017), "Thermal buckling and postbuckling of functionally graded graphene nanocomposite plates", *Mater. Des.*, **132**, 430-441. https://doi.org/10.1016/j.matdes.2017.07.025
Youcef, D.O., Abdelhakim, K., Benzair, A., Anis Bousahla, A. and Tounsi, A. (2018), "Dynamic analysis of nanoscale beams including surface stress effects", *Smart Struct. Syst., Int. J.*, **21**(1), 65-74. https://doi.org/10.12989/sss.2018.21.1.065
Zenkour, A.M. (2016), "Buckling of a single-layered graphene sheet embedded in visco-Pasternak's medium via nonlocal first-order theory", *Adv. Nano Res., Int. J.*, **4**(4), 309-326. https://doi.org/10.12989/anr.2016.4.4.309

CC

Appendix A

Extended nonlocal formulation of strain energy (U), foundation work (wf), work of biaxial loading (wb) and magnetic field work (wm) are expressed as

$$
\begin{aligned}
U = {} & \left(\frac{\partial}{\partial x}w_0\right)\kappa A_{55}\phi_1 + \left(\frac{\partial}{\partial y}w_0\right)\kappa_s A_{44}\phi_2 + \left(\frac{1}{2}\right)\left(\frac{\partial}{\partial x}u_0\right)A_{11}\left(\frac{\partial}{\partial x}w_0\right)^2 \\
& + \left(\frac{1}{2}\right)\left(\frac{\partial}{\partial x}u_0\right)A_{12}\left(\frac{\partial}{\partial y}w_0\right)^2 + \left(\frac{1}{2}\right)\left(\frac{\partial}{\partial x}\phi_1\right)B_{11}\left(\frac{\partial}{\partial x}w_0\right)^2 \\
& + \left(\frac{1}{2}\right)\left(\frac{\partial}{\partial x}\phi_1\right)B_{12}\left(\frac{\partial}{\partial y}w_0\right)^2 + \left(\frac{1}{2}\right)\left(\frac{\partial}{\partial x}w_0\right)^2 A_{12}\left(\frac{\partial}{\partial y}v_0\right) \\
& + \left(\frac{1}{2}\right)\left(\frac{\partial}{\partial x}w_0\right)^2 B_{12}\left(\frac{\partial}{\partial y}\phi_2\right) + \left(\frac{1}{4}\right)\left(\frac{\partial}{\partial x}w_0\right)^2 A_{12}\left(\frac{\partial}{\partial y}w_0\right)^2 \\
& + \left(\frac{1}{2}\right)\left(\frac{\partial}{\partial y}v_0\right)A_{22}\left(\frac{\partial}{\partial y}w_0\right)^2 + \left(\frac{1}{2}\right)\left(\frac{\partial}{\partial y}\phi_2\right)B_{22}\left(\frac{\partial}{\partial y}w_0\right)^2 \\
& + \left(\frac{1}{2}\right)\left(\frac{\partial}{\partial x}w_0\right)^2\left(\frac{\partial}{\partial y}w_0\right)^2 A_{66} + \left(\frac{1}{2}\right)\kappa_s A_{55}\left(\frac{\partial}{\partial x}w_0\right)^2 \\
& + \left(\frac{1}{2}\right)\kappa_s A_{55}(\phi_1)^2 + \left(\frac{1}{2}\right)\kappa_s A_{44}\left(\frac{\partial}{\partial y}w_0\right)^2 + \left(\frac{1}{2}\right)\kappa_s A_{44}(\phi_2)^2 \\
& + \left(\frac{\partial}{\partial x}u_0\right)B_{11}\left(\frac{\partial}{\partial x}\phi_1\right) + \left(\frac{\partial}{\partial x}u_0\right)A_{12}\left(\frac{\partial}{\partial y}v_0\right) + \left(\frac{\partial}{\partial x}u_0\right)B_{12}\left(\frac{\partial}{\partial y}\phi_2\right) \\
& + \left(\frac{\partial}{\partial x}\phi_1\right)B_{12}\left(\frac{\partial}{\partial y}v_0\right) + \left(\frac{\partial}{\partial x}\phi_1\right)D_{12}\left(\frac{\partial}{\partial y}\phi_2\right) + \left(\frac{1}{8}\right)\left(\frac{\partial}{\partial x}w_0\right)^4 A_{11} \\
& + \left(\frac{\partial}{\partial y}v_0\right)B_{22}\left(\frac{\partial}{\partial y}\phi_2\right) + \left(\frac{1}{8}\right)\left(\frac{\partial}{\partial y}w_0\right)^4 A_{22} + \left(\frac{1}{2}\right)D_{66}\left(\frac{\partial}{\partial y}\phi_1\right)^2 \\
& + \left(\frac{1}{2}\right)A_{11}\left(\frac{\partial}{\partial x}u_0\right)^2 + \left(\frac{1}{2}\right)D_{11}\left(\frac{\partial}{\partial x}\phi_1\right)^2 + \left(\frac{1}{2}\right)A_{22}\left(\frac{\partial}{\partial y}v_0\right)^2 \\
& + \left(\frac{1}{2}\right)D_{22}\left(\frac{\partial}{\partial y}\phi_2\right)^2 + \left(\frac{\partial}{\partial x}v_0\right)B_{66}\left(\frac{\partial}{\partial x}\phi_2\right) + \left(\frac{\partial}{\partial x}v_0\right)A_{66}\left(\frac{\partial}{\partial y}u_0\right)
\end{aligned}
\tag{A1}
$$

$$+\left(\frac{\partial}{\partial x}v_0\right)A_{66}\left(\frac{\partial}{\partial x}w_0\right)\left(\frac{\partial}{\partial y}w_0\right)+\left(\frac{\partial}{\partial x}v_0\right)B_{66}\left(\frac{\partial}{\partial y}\phi_1\right)$$
$$+\left(\frac{\partial}{\partial x}\phi_2\right)B_{66}\left(\frac{\partial}{\partial y}u_0\right)+\left(\frac{\partial}{\partial x}\phi_2\right)B_{66}\left(\frac{\partial}{\partial x}w_0\right)\left(\frac{\partial}{\partial y}w_0\right)$$
$$+\left(\frac{\partial}{\partial y}u_0\right)A_{66}\left(\frac{\partial}{\partial x}w_0\right)\left(\frac{\partial}{\partial y}w_0\right)+\left(\frac{\partial}{\partial x}\phi_2\right)D_{66}\left(\frac{\partial}{\partial y}\phi_1\right) \quad \text{(A1)}$$
$$+\left(\frac{\partial}{\partial x}w_0\right)\left(\frac{\partial}{\partial y}w_0\right)B_{66}\left(\frac{\partial}{\partial y}\phi_1\right)+\left(\frac{\partial}{\partial y}u_0\right)B_{66}\left(\frac{\partial}{\partial y}\phi_1\right)$$
$$+(1/2)A_{66}\left(\frac{\partial}{\partial y}u_0\right)^2+(1/2)A_{66}\left(\frac{\partial}{\partial x}v_0\right)^2+(1/2)D_{66}\left(\frac{\partial}{\partial x}\phi_2\right)^2,$$

$$w_f^{nl}=-K_w(w_0)^2+w_0G_p\left(\frac{\partial^2}{\partial x^2}w_0\right)+w_0G_p\left(\frac{\partial^2}{\partial y^2}w_0\right)+2\mu^2K_w\left(\frac{\partial}{\partial x}w_0\right)^2$$
$$+2\mu^2K_ww_0\left(\frac{\partial^2}{\partial x^2}w_0\right)-\mu^2\left(\frac{\partial^2}{\partial x^2}w_0\right)^2G_p-\mu^2w_0G_p\left(\frac{\partial^4}{\partial x^4}w_0\right)$$
$$-2\mu^2G_p\left(\frac{\partial}{\partial x}w_0\right)\left(\frac{\partial^3}{\partial x^3}w_0\right)-2\mu^2G_p\left(\frac{\partial^2}{\partial x^2}w_0\right)\left(\frac{\partial^2}{\partial y^2}w_0\right) \quad \text{(A2)}$$
$$-2\mu^2G_p\left(\frac{\partial}{\partial x}w_0\right)\left(\frac{\partial^3}{\partial y^2\partial x}w_0\right)-2\mu^2G_pw_0\left(\frac{\partial^4}{\partial y^2\partial x^2}w_0\right)$$
$$+2\mu^2K_w\left(\frac{\partial}{\partial y}w_0\right)^2+2\mu^2K_ww_0\left(\frac{\partial^2}{\partial y^2}w_0\right)-\mu^2G_p\left(\frac{\partial^2}{\partial y^2}w_0\right)^2$$
$$-2\mu^2G_p\left(\frac{\partial}{\partial y}w_0\right)\left(\frac{\partial^3}{\partial y\partial x^2}w_0\right)-2\mu^2G_p\left(\frac{\partial}{\partial y}w_0\right)\left(\frac{\partial^3}{\partial y^3}w_0\right)-\mu^2w_0G_p\left(\frac{\partial^4}{\partial y^4}w_0\right),$$

$$w_b^{nl}=\frac{1}{2}F\left(\frac{\partial}{\partial x}w\right)^2-\mu^2F\left(\frac{\partial}{\partial x}w\right)\left(\frac{\partial^3}{\partial x^3}w\right)-\mu^2F\left(\frac{\partial^2}{\partial y\partial x}w(x,y)\right)^2$$
$$-\mu^2F\left(\frac{\partial^2}{\partial x^2}w\right)^2-\mu^2F\left(\frac{\partial}{\partial x}w\right)\frac{\partial^3}{\partial y^2\partial x}w+\frac{1}{2}kF\left(\frac{\partial}{\partial y}w\right)^2-\mu^2kF\left(\frac{\partial^2}{\partial y\partial x}w\right)^2 \quad \text{(A3)}$$
$$-\mu^2kF\left(\frac{\partial}{\partial y}w\right)\frac{\partial^3}{\partial y\partial x^2}w-\mu^2kF\left(\frac{\partial^2}{\partial y^2}w\right)^2-\mu^2kF\left(\frac{\partial}{\partial y}w\right)\left(\frac{\partial^3}{\partial y^3}w\right),$$

$$w_m^{nl}=v_0\eta{H_x}^2\left(\frac{\partial^2}{\partial x^2}v_0\right)h+v_0\eta{H_x}^2\left(\frac{\partial^2}{\partial y^2}v_0\right)h+w_0\eta{H_x}^2\left(\frac{\partial}{\partial y}\phi_2\right)h$$
$$+w_0\eta{H_x}^2\left(\frac{\partial^2w_0}{\partial x^2}\right)h+\frac{1}{12}h^3w_0\left(\frac{\partial^3\phi_2}{\partial y\partial x^2}\right)\eta{H_x}^2+\frac{1}{12}h^3w_0\left(\frac{\partial^3\phi_2}{\partial y^3}\right)\eta{H_x}^2$$
$$-\mu^2v_0\eta{H_x}^2\left(\frac{\partial^4}{\partial x^4}v_0\right)h-2\mu^2v_0\eta{H_x}^2\left(\frac{\partial^4}{\partial y^2\partial x^2}v_0\right)h \quad \text{(A4)}$$
$$-\mu^2w_0\eta{H_x}^2\left(\frac{\partial^4}{\partial x^4}w_0\right)h-\frac{1}{12}\mu^2h^3w_0\left(\frac{\partial^5}{\partial y\partial x^4}\phi_2\right)\eta{H_x}^2$$
$$-\frac{1}{6}\mu^2h^3w_0\left(\frac{\partial^5}{\partial y^3\partial x^2}\phi_2\right)\eta{H_x}^2-\mu^2v_0\eta{H_x}^2\left(\frac{\partial^4}{\partial y^4}v_0\right)h$$

$$-\mu^2 w_0 \eta {H_x}^2 \left(\frac{\partial^3}{\partial y^3}\phi_2\right) h - \mu^2 w_0 \eta {H_x}^2 \left(\frac{\partial^4}{\partial y^2 \partial x^2} w_0\right) h$$
$$-\frac{1}{12}\mu^2 h^3 w_0 \left(\frac{\partial^5}{\partial y^5}\phi_2\right) \eta {H_x}^2 - \mu^2 w_0 \eta {H_x}^2 \left(\frac{\partial^3}{\partial y \partial x^2}\phi_2\right) h, \quad \text{(A4)}$$